

Search for $B \rightarrow \tau\nu$ and $B \rightarrow K\nu\bar{\nu}$

T. E. Browder,¹ Y. Li,¹ J. L. Rodriguez,¹ H. Yamamoto,¹ T. Bergfeld,² B. I. Eisenstein,² J. Ernst,² G. E. Gladding,² G. D. Gollin,² R. M. Hans,² E. Johnson,² I. Karliner,² M. A. Marsh,² M. Palmer,² C. Plager,² C. Sedlack,² M. Selen,² J. J. Thaler,² J. Williams,² K. W. Edwards,³ R. Janicek,⁴ P. M. Patel,⁴ A. J. Sadoff,⁵ R. Ammar,⁶ A. Bean,⁶ D. Besson,⁶ R. Davis,⁶ N. Kwak,⁶ X. Zhao,⁶ S. Anderson,⁷ V. V. Frolov,⁷ Y. Kubota,⁷ S. J. Lee,⁷ R. Mahapatra,⁷ J. J. O'Neill,⁷ R. Poling,⁷ T. Riehle,⁷ A. Smith,⁷ C. J. Stepaniak,⁷ J. Urheim,⁷ S. Ahmed,⁸ M. S. Alam,⁸ S. B. Athar,⁸ L. Jian,⁸ L. Ling,⁸ M. Saleem,⁸ S. Timm,⁸ F. Wappler,⁸ A. Anastassov,⁹ J. E. Duboscq,⁹ E. Eckhart,⁹ K. K. Gan,⁹ C. Gwon,⁹ T. Hart,⁹ K. Honscheid,⁹ D. Hufnagel,⁹ H. Kagan,⁹ R. Kass,⁹ T. K. Pedlar,⁹ H. Schwarthoff,⁹ J. B. Thayer,⁹ E. von Toerne,⁹ M. M. Zoeller,⁹ S. J. Richichi,¹⁰ H. Severini,¹⁰ P. Skubic,¹⁰ A. Undrus,¹⁰ S. Chen,¹¹ J. Fast,¹¹ J. W. Hinson,¹¹ J. Lee,¹¹ D. H. Miller,¹¹ E. I. Shibata,¹¹ I. P. J. Shipsey,¹¹ V. Pavlunin,¹¹ D. Cronin-Hennessy,¹² A. L. Lyon,¹² E. H. Thorndike,¹² C. P. Jessop,¹³ H. Marsiske,¹³ M. L. Perl,¹³ V. Savinov,¹³ D. Ugolini,¹³ X. Zhou,¹³ T. E. Coan,¹⁴ V. Fadeyev,¹⁴ Y. Maravin,¹⁴ I. Narsky,¹⁴ R. Stroynowski,¹⁴ J. Ye,¹⁴ T. Wlodek,¹⁴ M. Artuso,¹⁵ R. Ayad,¹⁵ C. Boulahouache,¹⁵ K. Bukin,¹⁵ E. Dambasuren,¹⁵ S. Karamov,¹⁵ G. Majumder,¹⁵ G. C. Moneti,¹⁵ R. Mountain,¹⁵ S. Schuh,¹⁵ T. Skwarnicki,¹⁵ S. Stone,¹⁵ G. Viehhauser,¹⁵ J. C. Wang,¹⁵ A. Wolf,¹⁵ J. Wu,¹⁵ S. Kopp,¹⁶ A. H. Mahmood,¹⁷ S. E. Csorna,¹⁸ I. Danko,¹⁸ K. W. McLean,¹⁸ Sz. Márka,¹⁸ Z. Xu,¹⁸ R. Godang,¹⁹ K. Kinoshita,^{19,*} I. C. Lai,¹⁹ S. Schrenk,¹⁹ G. Bonvicini,²⁰ D. Cinabro,²⁰ S. McGee,²⁰ L. P. Perera,²⁰ G. J. Zhou,²⁰ E. Lipeles,²¹ S. P. Pappas,²¹ M. Schmidler,²¹ A. Shapiro,²¹ W. M. Sun,²¹ A. J. Weinstein,²¹ F. Würthwein,^{21,†} D. E. Jaffe,²² G. Masek,²² H. P. Paar,²² E. M. Potter,²² S. Prell,²² V. Sharma,²² D. M. Asner,²³ A. Eppich,²³ T. S. Hill,²³ R. J. Morrison,²³ R. A. Briere,²⁴ T. Ferguson,²⁴ H. Vogel,²⁴ B. H. Behrens,²⁵ W. T. Ford,²⁵ A. Gritsan,²⁵ J. Roy,²⁵ J. G. Smith,²⁵ J. P. Alexander,²⁶ R. Baker,²⁶ C. Bebek,²⁶ B. E. Berger,²⁶ K. Berkelman,²⁶ F. Blanc,²⁶ V. Boisvert,²⁶ D. G. Cassel,²⁶ M. Dickson,²⁶ P. S. Drell,²⁶ K. M. Ecklund,²⁶ R. Ehrlich,²⁶ A. D. Foland,²⁶ P. Gaidarev,²⁶ L. Gibbons,²⁶ B. Gittelman,²⁶ S. W. Gray,²⁶ D. L. Hartill,²⁶ B. K. Heltsley,²⁶ P. I. Hopman,²⁶ C. D. Jones,²⁶ D. L. Kreinick,²⁶ M. Lohner,²⁶ A. Magerkurth,²⁶ T. O. Meyer,²⁶ N. B. Mistry,²⁶ E. Nordberg,²⁶ J. R. Patterson,²⁶ D. Peterson,²⁶ D. Riley,²⁶ J. G. Thayer,²⁶ P. G. Thies,²⁶ D. Urner,²⁶ B. Valant-Spaight,²⁶ A. Warburton,²⁶ P. Avery,²⁷ C. Prescott,²⁷ A. I. Rubiera,²⁷ J. Yelton,²⁷ J. Zheng,²⁷ G. Brandenburg,²⁸ A. Ershov,²⁸ Y. S. Gao,²⁸ D. Y.-J. Kim,²⁸ and R. Wilson²⁸

(CLEO Collaboration)

¹University of Hawaii at Manoa, Honolulu, Hawaii 96822

²University of Illinois, Urbana-Champaign, Illinois 61801

³Carleton University, Ottawa, Ontario, Canada K1S 5B6
and the Institute of Particle Physics, Canada

⁴McGill University, Montréal, Québec, Canada H3A 2T8
and the Institute of Particle Physics, Canada

⁵Ithaca College, Ithaca, New York 14850

⁶University of Kansas, Lawrence, Kansas 66045

⁷University of Minnesota, Minneapolis, Minnesota 55455

⁸State University of New York at Albany, Albany, New York 12222

⁹The Ohio State University, Columbus, Ohio 43210

¹⁰University of Oklahoma, Norman, Oklahoma 73019

¹¹Purdue University, West Lafayette, Indiana 47907

¹²University of Rochester, Rochester, New York 14627

¹³Stanford Linear Accelerator Center, Stanford University, Stanford, California 94309

¹⁴Southern Methodist University, Dallas, Texas 75275

¹⁵Syracuse University, Syracuse, New York 13244

¹⁶University of Texas, Austin, Texas 78712

¹⁷University of Texas–Pan American, Edinburg, Texas 78539

¹⁸Vanderbilt University, Nashville, Tennessee 37235

¹⁹Virginia Polytechnic Institute and State University, Blacksburg, Virginia 24061

²⁰Wayne State University, Detroit, Michigan 48202

²¹California Institute of Technology, Pasadena, California 91125

²²University of California, San Diego, La Jolla, California 92093

²³University of California, Santa Barbara, California 93106

²⁴Carnegie Mellon University, Pittsburgh, Pennsylvania 15213

²⁵University of Colorado, Boulder, Colorado 80309-0390

²⁶Cornell University, Ithaca, New York 14853²⁷University of Florida, Gainesville, Florida 32611²⁸Harvard University, Cambridge, Massachusetts 02138

(Received 26 July 2000)

We report results of a search for $B \rightarrow \tau\nu$ in a sample of 9.7×10^6 charged B meson decays. We exclusively reconstruct the companion \bar{B} decay to suppress background. We set an upper limit on the branching fraction $\mathcal{B}(B \rightarrow \tau\nu) < 8.4 \times 10^{-4}$ at 90% confidence level. We also establish $\mathcal{B}(B^\pm \rightarrow K^\pm \nu\bar{\nu}) < 2.4 \times 10^{-4}$ at 90% confidence level.

DOI: 10.1103/PhysRevLett.86.2950

PACS numbers: 13.20.He, 14.40.Nd, 14.60.Fg

The purely leptonic decay of the B meson offers a clean probe of the weak decay process. The branching fraction,

$$\mathcal{B}(B \rightarrow \ell\nu) = \frac{G_F^2 m_B m_\ell^2}{8\pi} \left(1 - \frac{m_\ell^2}{m_B^2}\right)^2 f_B^2 |V_{ub}|^2 \tau_B,$$

exhibits simple dependence on the meson decay constant f_B and the quark mixing matrix element V_{ub} . V_{ub} quantifies the mixing between the heavy b and light u quark mass eigenstates in the weak interaction, and as such is a fundamental parameter. The dependence on lepton mass (m_ℓ) arises from helicity conservation and heavily suppresses the rate to light leptons. In the B system this means $\tau\nu$ is favored over $\mu\nu$ or $e\nu$ final states. Nevertheless, the expected branching fraction $\mathcal{B}(B \rightarrow \tau\nu) \sim (0.2 - 1) \times 10^{-4}$ is small and the presence of additional neutrinos in the final state significantly weakens the experimental signature.

In the context of the standard model, a crisp determination of quark mixing matrix parameters may be obtained in principle by comparing $\mathcal{B}(B \rightarrow \tau\nu)$ with the difference in heavy and light neutral B_d masses [1],

$$\Delta m_d = \frac{G_F^2}{6\pi^2} \eta_B m_B m_W^2 f_B^2 S_0(x_t) |V_{td}|^2,$$

a quantity which is known from B_d mixing measurements [2] to considerable precision: $\Delta m_d = 0.464 \pm 0.18 \text{ ps}^{-1}$. In this comparison the dependence on the poorly known decay constant f_B drops out, and one obtains [3]

$$\mathcal{B}(B \rightarrow \tau\nu) = [(4.08 \pm 0.24) \times 10^{-4}] \left| \frac{V_{ub}}{V_{td}} \right|^2.$$

The range ± 0.24 is set by current theoretical uncertainties. Given a sufficiently precise experimental measurement of the branching fraction, this relationship could be used to map out an allowed zone in the plane of Wolfenstein ρ and η parameters [4] that is roughly similar to that determined by measurements of $|V_{ub}|$, but subject to a different mix of statistical, systematic, and theoretical uncertainties [5]. Alternatively, if $|V_{ub}|$ is taken from other measurements in the B system, then the determination of $\mathcal{B}(B \rightarrow \tau\nu)$ may be viewed as a measurement of the decay constant f_B . This may be the only way to measure f_B . Looking beyond the standard model, the $B \rightarrow \tau\nu$ rate is sensitive to effects from charged Higgs bosons and may be used to set a limit on charged Higgs mass. The sensitivity is greatest for large values of the Higgs doublet vacuum expectation value ratio, $\tan\beta$ [6].

Existing experimental information is limited, however. A previous search by this collaboration [7] in the $Y(4S) \rightarrow B\bar{B}$ system yielded a 90% confidence level upper limit $\mathcal{B}(B \rightarrow \tau\nu) < 22 \times 10^{-4}$, and three searches [8] in the $Z^0 \rightarrow b\bar{b}$ system have yielded upper limits ranging from 16×10^{-4} down to 5.7×10^{-4} . Although the Z^0 system offers powerful kinematical advantages, future measurements will be at the $Y(4S)$.

In this Letter we present results of a new search for $B \rightarrow \tau\nu$ using a method which is uniquely adapted to the $Y(4S)$ system. In this method we fully reconstruct the companion B in a quasi-inclusive reconstruction technique similar to that used for earlier measurements [9].

The data used in this analysis were collected with the CLEO II detector at the Cornell Electron Storage Ring (CESR). The data sample consists of 9.13 fb^{-1} taken at the $Y(4S)$, corresponding to $9.66 \text{ M } B\bar{B}$ pairs, and an additional 4.35 fb^{-1} taken below the $B\bar{B}$ threshold, which is used for background studies.

CLEO II is a general purpose solenoidal magnet detector, described in detail elsewhere [10]. Cylindrical drift chambers in a 1.5 T solenoidal magnetic field measure momentum and specific ionization (dE/dx) of charged particles. Photons are detected using a 7800-crystal CsI(Tl) electromagnetic calorimeter covering 98% of 4π . Two-thirds of the data was taken in the CLEO II.V detector configuration, in which the innermost chamber was replaced by a three-layer, double-sided silicon vertex detector, and the gas in the main drift chamber was changed from an argon-ethane to a helium-propane mixture.

Track quality requirements are imposed on charged tracks, and pions and kaons are identified by their specific ionization, dE/dx . Pairs of photons with an invariant mass within 2.5 standard deviations of the nominal π^0 mass are kinematically fit with a π^0 mass constraint. K^0 mesons are identified in the $K_S^0 \rightarrow \pi^+\pi^-$ decay mode. Electrons are identified based on dE/dx and the ratio of the shower energy in the CsI calorimeter to track momentum. Muons over about 1 GeV/ c momentum are identified by their penetration depth in the instrumented steel flux return; below about 1 GeV/ c muons are not distinguished from pions.

The experiment is fully simulated by a GEANT-based Monte Carlo [11] that includes beam-related debris by overlaying random trigger events on Monte Carlo generated events. The simulation is used to study backgrounds

and optimize selection criteria, but directly enters the analysis only through the calculation of the signal reconstruction efficiency.

To search for $B \rightarrow \tau\nu$ decays we fully reconstruct each $Y(4S) \rightarrow B^+B^-$ event in the simultaneous decay modes $B^+ \rightarrow \tau^+\nu$ (“signal B ”) and $B^- \rightarrow D^{(*)0}(n\pi)^-$ (“companion B ”). Here and throughout, charge conjugate modes are implied.

For the signal B we accept any single track which passes quality requirements and is identified as a lepton or pion. Pion candidates must have momentum greater than 0.7 GeV/ c and must neither pass lepton identification criteria nor be candidate K_S^0 daughters. This approach encompasses the three decay modes $\tau \rightarrow (e, \mu)\nu\bar{\nu}$ and $\tau \rightarrow \pi\nu$, which together constitute 46.5% of the τ branching fraction. Reconstruction efficiencies are 64%, 34%, and 84%, respectively, and there is some cross feed into the “ $\pi\nu$ ” channel from the tau decay modes $e\nu\bar{\nu}$, $\mu\nu\bar{\nu}$, and $\rho\nu$. The cross feed efficiencies are 6%, 20%, and 8%, respectively. The total τ reconstruction efficiency, including τ branching fractions and cross feeds, is 32.9%.

For the companion B , we take advantage of the large (46%) $b \rightarrow c\bar{u}\bar{d}$ branching fraction and reconstruct $B^- \rightarrow D^{(*)0}(n\pi)^-$, accepting either D^0 or $D^{*0} \rightarrow D^0(\gamma, \pi^0)$ and reconstructing the D^0 in the following eight modes: $K^-\pi^+$, $K^-\pi^+\pi^0$, $K^-\pi^+\pi^-\pi^+$, $\bar{K}^0\pi^+\pi^-$, $K^-\pi^+\pi^0\pi^0$, $K^-\pi^+\pi^-\pi^+\pi^0$, $\bar{K}^0\pi^+\pi^-\pi^0$, and $\bar{K}^0\pi^0$. Based on the reconstructed D^0 mass, the π^0 mass, and the kaon and pion particle identification information, we compute a χ^2 quality factor and use it to reject poor D^0 candidates. The $(n\pi)^-$ system may be any of the following: π^- , $\pi^-\pi^+\pi^-$, $\pi^-\pi^+\pi^-\pi^+\pi^-$, $\pi^-\pi^0$, $\pi^-\pi^+\pi^-\pi^0$, or $\pi^-\pi^0\pi^0$.

With each B reconstructed in one of the target decay modes, we now require that there be no additional charged tracks in the detector, and that the sum of all energy in the crystal calorimeter not clustered with the energy deposition of reconstructed charged tracks or π^0 s be less than a mode-dependent value E_{\max} . For the clean decay modes of the companion B , $B^+ \rightarrow D^{(*)0}\pi^+$ and $B^+ \rightarrow D^{(*)0}\pi^+\pi^0$, we set $E_{\max} = 0.6$ GeV, while for all other modes it is tightened to 0.4 GeV. The main source of nonassociated calorimeter energy deposition is from hadronic interactions in the calorimeter that cast debris laterally and result in small energy deposits that are not matched with a parent track. Monte Carlo simulation and careful investigation of appropriate data samples indicate that on average such deposits sum to 240 MeV per (signal) event. Additional contributions arise from beam-related debris, averaging 26 MeV per event and concentrated in the far forward and backward portions of the calorimeter; and from real photons from incorrect signal reconstruction, which average 10 MeV per event. In addition to this summed energy requirement, we also test whether any unassigned calorimeter signal can be paired with an already identified photon shower to form an object with invariant mass within

2.5 standard deviations of the π^0 mass. If such a pairing can be made, the event is rejected.

We suppress background from $B\bar{B}$ events by imposing requirements on the value of q^2 , the invariant mass squared of the $n\pi$ system. For most of the $n\pi$ states we demand $q^2 < 2.0$ GeV², but for the case $n\pi = \pi^+$ no restriction is needed, and for $n\pi = \pi^+\pi^-\pi^+\pi^0$ we permit $q^2 < 2.5$ GeV². The selection criteria described above have an overall signal efficiency of approximately 50%.

Backgrounds arising from $e^+e^- \rightarrow q\bar{q}$ events (“continuum”) are distinguished by a jetty topology. To suppress these backgrounds we compute the direction of the thrust axis of the companion B candidate and measure the angle θ to the direction of the lepton or pion of the τ candidate. For a signal event these directions are uncorrelated, while for continuum background the correlation is high and the $|\cos\theta|$ distribution peaks at 1. We require $|\cos\theta|$ be less than 0.90 and 0.75 for $\tau \rightarrow \ell\nu\bar{\nu}$ and $\tau \rightarrow \pi\nu$ candidates, respectively. Continuum background is more severe in the $\pi\nu$ mode and demands a tighter cut. Additional backgrounds from $e^+e^- \rightarrow \tau^+\tau^-$ are suppressed by requiring the Fox-Wolfram [12] moments ratio $H2/H0$ to be less than 0.5. Contributions from two-photon events ($e^+e^- \rightarrow \gamma^{(*)}e^+e^-$) are negligible.

The identification of acceptable candidates for the τ daughter, the D^0 , and $n\pi$ system, together with the absence of extra tracks or significant extra neutral energy, marks the appearance of a signal candidate. We now characterize these candidates by the kinematic properties of the companion B , since there is no additional information in the lone τ daughter track. In particular, we use the total momentum \vec{P}_B and energy E_B of the companion B , computed from momenta and energies of its daughter products. These raw quantities are then recast as the more useful beam-constrained mass $M(B) \equiv (E_{\text{beam}}^2 - \vec{P}_B)^{1/2}$ and energy difference $\Delta E \equiv E_B - E_{\text{beam}}$ variables. If more than one candidate is reconstructed in a given event, the one with the highest value of ΔE is selected.

Figure 1 shows the distribution of events in the ΔE - $M(B)$ plane for Monte Carlo $B\bar{B}$ background, Monte Carlo continuum background, Monte Carlo signal, and for the actual data set. The Monte Carlo background samples represent equivalent integrated luminosity of, respectively, 3 times and 2 times the actual data sample. The clustering of signal Monte Carlo events inside the $M(B)$ signal region but around $\Delta E \sim -0.2$ GeV is due to reconstructing $B^- \rightarrow D^{*0}(n\pi)^-$ as $B^- \rightarrow D^0(n\pi)^-$. In such cases, the absence of the appropriate soft π^0 or γ from D^{*0} decay lowers the candidate’s total energy. Events in this satellite peak constitute 24% of the total signal yield.

We select events whose $M(B)$ falls within 2.5 standard deviations of the true B mass, and extract the signal yield by fitting the resulting ΔE distribution. The net signal efficiency including all secondary branching fractions for the analysis is $\varepsilon = 0.69 \times 10^{-3}$. The signal fit shape is the sum of a narrow ($\sigma = 24$ MeV) Gaussian centered at

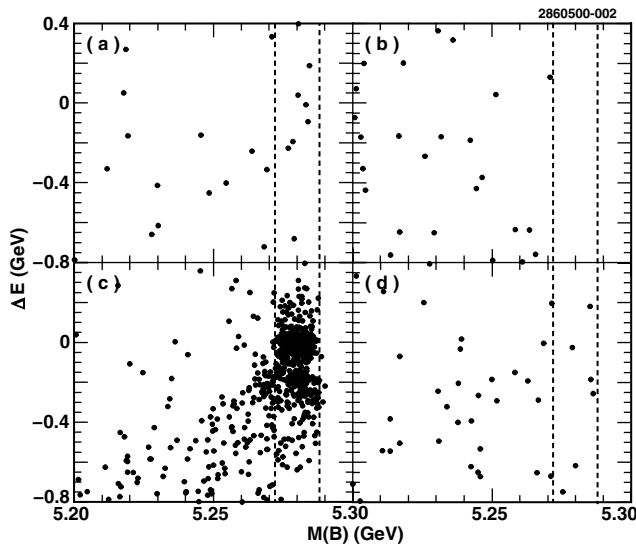


FIG. 1. Distributions in ΔE (vertical axis) and $M(B)$ (horizontal axis). (a) $B\bar{B}$ Monte Carlo; (b) continuum Monte Carlo; (c) signal Monte Carlo; (d) data. The dashed lines delineate the signal region.

$\Delta E = 0$ for the primary signal yield, and a wide Gaussian ($\sigma = 115$ MeV) centered at $\Delta E = -164$ MeV for the D^{*0} satellite peak. The shapes and the relative normalization of these Gaussians are determined by Monte Carlo. Residual backgrounds are modeled by a linear distribution whose slope is determined by fitting the data lying outside the 2.5σ window in $M(B)$. We fit the ΔE distribution by an extended unbinned maximum likelihood method [13] to obtain the total yield of signal and background; the ΔE shape parameters are fixed by the procedure described above and are not varied in the fit. The systematic error in signal yield associated with the uncertainty in the background shape is 4%. Figure 2a shows the final ΔE distribution of data inside the 2.5 standard deviation signal region of $M(B)$. Six events remain after all selection criteria are applied, three consistent with leptonic tau decay, three with pionic decay. Figure 2b shows the fit shape with normalization as resulting from the likelihood fit; the central value of the fitted yield is 0.96 events.

The background level is consistent with Monte Carlo expectations given the selection criteria and the size of the data sample. Figure 2c shows a comparison of the ΔE distribution for Monte Carlo events and data. To increase the yield for this plot we have released the restriction on leftover tracks, and here require exactly one extra charged track. These data events are thus in a sideband to the signal region. There are 71 such events in data, and 68 predicted by Monte Carlo. As evident in the figure, the Monte Carlo also reproduces the ΔE spectrum of these events very closely. Examination of Monte Carlo background events in the signal region itself shows (a) that the background is composed of approximately equal amounts of $B\bar{B}$ and continuum events; (b) that the background in the

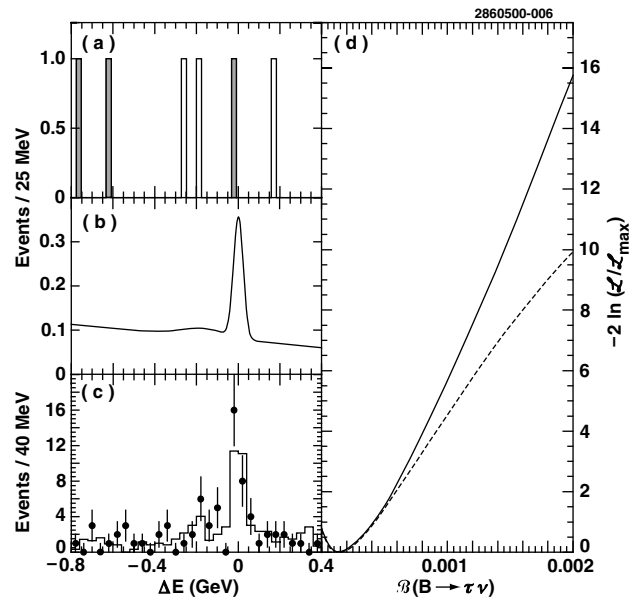


FIG. 2. Final results. (a) The six events fitted. Shaded entries correspond to candidates which are simultaneously $K^\pm \nu \bar{\nu}$ candidates. (b) The fit shape with normalizations as resulting from the fit. (c) Distribution in ΔE of Monte Carlo (solid) and data (points) for events with exactly one extra charged track. (d) $-2 \ln \mathcal{L} / \mathcal{L}_{\max}$ versus $\mathcal{B}(B \rightarrow \tau\nu)$. Solid: statistical errors only; dotted: systematic errors included as described in text.

$\tau \rightarrow \pi\nu$ mode is dominated by continuum while the background in the $\tau \rightarrow \ell\nu\bar{\nu}$ mode is dominated by $B\bar{B}$; and (c) about 75% of all background events, whether $B\bar{B}$ or continuum, have a K_L present. Were it available, hadronic calorimetry would help suppress some of this remaining background.

The branching ratio is related to the signal yield N_{sig} by $\mathcal{B}(B \rightarrow \tau\nu) = N_{\text{sig}} / N_{B\bar{B}} \epsilon$ where $N_{B\bar{B}} = 9.66 \times 10^6$ is the number of charged B mesons in the data sample and ϵ is the efficiency as given above. We cross-check the efficiency by conducting a separate analysis identical to this one in all key respects except that the $\tau\nu$ target signal is replaced by $D^{*0} \ell^- \nu$ whose branching fraction is large and well measured. To ensure as much topological similarity to the $\tau\nu$ case as possible, we restrict this ancillary analysis to the low-multiplicity submode, $D^0 \rightarrow K^- \pi^+$. We find a yield of $N(D^{*0} \ell^- \nu)_{\text{data}} = 43.1 \pm 8.4$ events in data, and compare this to the Monte Carlo result $N(D^{*0} \ell^- \nu)_{\text{MC}} = 30.4 \pm 4.3$ where the error is primarily due to uncertainties in the $B^- \rightarrow D^{*0} \ell^- \nu$ branching ratio [2]. The discrepancy between these yields is 1.3σ . We adopt a conservative course, using the efficiency determined by Monte Carlo, and assigning to it a relative systematic error given by $\delta\epsilon/\epsilon \equiv \sqrt{(4.3/30.4)^2 + (8.4/43.1)^2} = 24.1\%$.

Figure 2d shows the likelihood function (\mathcal{L}) plotted as $-2 \ln \mathcal{L} / \mathcal{L}_{\max}$ versus $\mathcal{B}(B \rightarrow \tau\nu)$. Also shown is the result of convolving the likelihood function with the systematic uncertainty distribution of the efficiency (assumed to be Gaussian). The systematic error on the efficiency is

dominated by the 24.1% discussed above, but also includes contributions from reconstruction efficiency uncertainty and uncertainty in the efficiency of the nonassociated neutral energy cuts. In total, the relative systematic error on efficiency is 24.4%. We integrate the systematics-convolved likelihood function to obtain a 90% confidence upper limit \mathcal{B}_{90} on $\mathcal{B}(B \rightarrow \tau\nu)$ from $0.90 = \int_0^{\mathcal{B}_{90}} \mathcal{L}(\mathcal{B}) d\mathcal{B} / \int_0^1 \mathcal{L}(\mathcal{B}) d\mathcal{B}$. We find

$$\mathcal{B}(B \rightarrow \tau\nu) < 8.4 \times 10^{-4}$$

at 90% confidence level. This approach can be shown [14] to be equivalent to the assumption of a flat Bayesian prior probability for $\mathcal{B}(B \rightarrow \tau\nu)$ and is known to yield a conservative upper limit. A frequentist approach based on generating Monte Carlo experiments gives $\mathcal{B}(B \rightarrow \tau\nu) < 7.4 \times 10^{-4}$ at 90% confidence level [15].

We also investigate the decay mode $B^\pm \rightarrow K^\pm \nu \bar{\nu}$ [16]. There is currently no experimental information on this decay mode, although limits on the related decay modes $B \rightarrow X_s \nu \bar{\nu}$ and $B \rightarrow K^{*0} \nu \bar{\nu}$ exist [17]. All these modes probe the quark mixing parameter $|V_{ts}|$, and the fully inclusive mode in particular offers a theoretically pristine approach to this fundamental quantity [1]. The search strategy is the same as described above, but we require that the lone track on the signal side fail lepton identification and be consistent with a kaon. The expected momentum distribution of the K^\pm peaks at ~ 2.5 GeV/ c , so we retain the 0.7 GeV/ c momentum requirement previously applied to the pion candidate in the $\pi\nu$ mode. The resulting set of three $K^\pm \nu \bar{\nu}$ signal candidates is a subset of the six $\tau\nu$ candidates. They are marked by shading in Fig. 2. We perform the same unbinned likelihood fit as above and obtain a central value yield of 0.81 events. The efficiency of the $K^\pm \nu \bar{\nu}$ is $\varepsilon = 1.8 \times 10^{-3}$; we find $\mathcal{B}(B^\pm \rightarrow K^\pm \nu \bar{\nu}) < 2.4 \times 10^{-4}$ at 90% confidence level. The efficiency is calculated using the form factor model of Ref. [16], but it changes only negligibly if instead we use three-body phase space and a constant matrix element. We corroborate our result with an independent analysis, which is based only on counting events and yields an upper limit $\mathcal{B}(B^\pm \rightarrow K^\pm \nu \bar{\nu}) < 6.6 \times 10^{-4}$ at 90% confidence level. As with the $\tau\nu$ analysis described above, the systematic error is dominated by the 24% relative uncertainty in the efficiency to reconstruct the companion B , and is included in the same manner. Systematic uncertainty due to background shape is only 2%.

We have reported an analysis of 9.66×10^6 charged B meson decays which results in a conservative upper limit on the branching fraction $\mathcal{B}(B \rightarrow \tau\nu) < 8.4 \times 10^{-4}$. We also modify the analysis slightly to establish $\mathcal{B}(B^\pm \rightarrow K^\pm \nu \bar{\nu}) < 2.4 \times 10^{-4}$. The method used is optimized for

conditions available at Y(4S) experiments, and we anticipate useful application of the method to other rare decay modes with large missing energy.

We gratefully acknowledge the effort of the CESR staff in providing us with excellent luminosity and running conditions. This work was supported by the National Science Foundation, the U.S. Department of Energy, the Research Corporation, the Natural Sciences and Engineering Research Council of Canada, the A. P. Sloan Foundation, the Swiss National Science Foundation, and Alexander von Humboldt Stiftung.

*Permanent address: University of Cincinnati, Cincinnati, OH 45221.

†Permanent address: Massachusetts Institute of Technology, Cambridge, MA 02139.

- [1] A. J. Buras and R. Fleischer, in *Heavy Flavours II*, edited by A. J. Buras and M. Lindner (World Scientific, Singapore, 1997).
- [2] PDG Collaboration, C. Caso *et al.*, *Eur. Phys. C* **3**, 1 (1998).
- [3] T. Draper, *Nucl. Phys. Proc. Suppl.* **73**, 43 (1999); B. H. Behrens *et al.*, *Phys. Rev. D* **61**, 052001 (2000).
- [4] L. Wolfenstein, *Annu. Rev. Nucl. Part. Sci.* **36**, 137 (1986).
- [5] G. Harris and J. Rosner, *Phys. Rev. D* **45**, 946 (1992).
- [6] W.-S. Hou, *Phys. Rev. D Brief Report* **48**, 2342 (1993).
- [7] CLEO Collaboration, M. Artuso *et al.*, *Phys. Lett. D* **47**, 785 (1995).
- [8] ALEPH Collaboration, D. Buskulic *et al.*, *Phys. Lett. B* **343**, 444 (1995); L3 Collaboration, M. Acciarri *et al.*, *Phys. Lett. B* **396**, 327 (1997); DELPHI Collaboration, P. Abreu *et al.*, Report No. CERN-EP/99-162.
- [9] CLEO Collaboration, H. Kroha *et al.*, in *Proceedings of the XXVIth International Conference on High Energy Physics, Dallas, 1992* (AIP, New York, 1993); CLEO Collaboration, M. S. Alam *et al.*, *Phys. Rev. Lett.* **74**, 2885 (1995); CLEO Collaboration, M. S. Alam *et al.*, Report No. CLEO-CONF 98-17, ICHEP98-1011; CLEO Collaboration, T. E. Browder *et al.*, *Phys. Rev. Lett.* **81**, 1786 (1998).
- [10] CLEO Collaboration, Y. Kubota *et al.*, *Nucl. Instrum. Methods Phys. Res., Sect. A* **320**, 66 (1992); T. S. Hill, *Nucl. Instrum. Methods Phys. Res., Sect. A* **418**, 32 (1998).
- [11] R. Brun *et al.*, GEANT 3.15, CERN DD/EE/84-1.
- [12] G. Fox and S. Wolfram, *Phys. Rev. Lett.* **41**, 1581 (1978).
- [13] L. Lyons, W. Allison, and J. Panella Comellas, *Nucl. Instrum. Methods Phys. Res., Sect. A* **245**, 530 (1986); R. Barlow, *Nucl. Instrum. Methods Phys. Res., Sect. A* **297**, 496 (1990).
- [14] G. Feldman and R. Cousins, *Phys. Rev. D* **57**, 3873 (1998).
- [15] I. Narsky, hep-ex/9904025.
- [16] P. Colangelo *et al.*, *Phys. Lett. B* **395**, 339 (1997).
- [17] ALEPH Collaboration, P. Perrodo *et al.*, Report No. ICHEP96 (PA-10-019); DELPHI Collaboration, W. Adam *et al.*, *Z. Phys. C* **72**, 207 (1996).